Handling Sideband Radiations in Time-Modulated Arrays Through Particle Swarm Optimization

Lorenzo Poli, Paolo Rocca, Luca Manica, and Andrea Massa

***Abstract*—The minimization of the power losses in time-modulated arrays is addressed by means of a suitable strategy based on particle swarm optimization. By properly modifying the modulation sequence, the method is aimed at reducing the amount of wasted power, analytically computed through a very effective closed-form relationship, while constraining the radiation pattern at the carrier frequency below a fixed sidelobe level. Representative results are reported and compared with previously published solutions to assess the effectiveness of the proposed approach.**

***Index Terms*—Linear arrays, pattern synthesis, time-modulated arrays.**

I. Introduction

The use of time as an additional degree of freedom in array synthesis has been investigated in the pioneering work by Shanks and Bickmore [1]. Kummer *et al.* in [2] discussed the possibility of using RF switches for modulating in time the element excitations in order to obtain average low and ultra-low side lobes. Successively, only a few works (e.g., [3]) have dealt with time modulation. As pointed out in [2], [4], the main difficulties to the diffusion of such a technique lie in its technical implementation. However, some recent prototypes [5], [6] and new interesting applications (e.g., the synthesis of sum and difference patterns [7] or the realization of phase switched screens [6]) have renewed the interest on time-modulated arrays as well as on its practical feasibility.

By a theoretical point of view, the modulation of the array excitations with RF switches generates undesired harmonic radiations and power losses. In order to reduce sideband radiations (SRs), different stochastic iterative algorithms have been proposed [5], [8]–[10]. They are based on the minimization of the sideband levels (SBLs) at the higher order harmonics. However, such a guideline presents some disadvantages. First, it enforces an "indirect" SRs reduction (i.e., through SBLs minimization). Moreover, it needs the computation of the SBL at each harmonic frequency. As a matter of fact, neglecting some higher harmonics and considering just low orders could prevent a suitable SR reduction. In order to overcome these drawbacks, this communication presents an innovative approach based on a Particle Swarm Optimizer (PSO) [11] aimed at synthesizing a desired pattern with a prescribed sidelobe level (SLL) at the carrier frequency also directly minimizing the power losses due to SRs. Towards this end, the closed-form relationship, derived in [4] to quantify the total power wasted in sideband radiations, is profitably exploited because of its analytic form, its simplicity, and to avoid the evaluation of the (infinite) set of higher harmonic patterns.

The outline of the communication is as follows. In Section II, the key-issues concerned with time-modulation for the array synthesis are briefly summarized. Successively, the PSO-based strategy for the reduction of the power losses due to SRs is described. Section III is devoted to the numerical analysis. Preliminary results are reported and compared with state-ofthe-art solutions to point out the effectiveness of the proposed approach. Finally, some conclusions are drawn (Section IV).

Manuscript received May 01, 2009; revised August 02, 2009. Date of manuscript acceptance September 15, 2009; date of publication January 26, 2010; date of current version April 07, 2010.

The authors are with the ELEDIA Research Group, Department of Information Engineering and Computer Science, University of Trento, 38050 Trento, Italy (e-mail: lorenzo.poli@disi.unitn.it; paolo.rocca@disi.unitn.it; paolo.rocca@dit.unitn.it; luca.manica@disi.unitn.it; andrea.massa@ing.unitn.it; http://www.eledia.ing.unitn.it).

Color versions of one or more of the figures in this communication are available online at http://ieeexplore.ieee.org.

Digital Object Identifier 10.1109/TAP.2010.2041165

II. Mathematical Formulation

Let us consider a time-modulated linear array of N (without loss of generality) isotropic elements located at $z_n = nd$, $n = 0, \ldots, N-1$, (d being the inter-element distance) along the z axis. The corresponding array factor is given by [2]

$$F(\theta, t) = e^{j\omega_0 t} \sum_{n=0}^{N-1} I_n(t) e^{jnu} \tag{1}$$

where $\omega_0 = 2\pi f_0$ is the carrier angular frequency, $u = (\omega_0/c) d \cos\theta$, c being the speed of light in vacuum, and θ the angle measured from the array axis. Moreover, $I_n(t) = \alpha_n U_n(t)$, $n = 0, \ldots, N-1$, are the time-modulated excitations. More specifically, $\underline{\alpha} = \{\alpha_n; n = 0, \ldots, N-1\}$ and $\underline{U}(t) = \{U_n(t); n = 0, \ldots, N-1\}$ are the set of static excitations and time-step functions of the RF switches, respectively.

Because of the periodicity of the pulse sequences, $U_n(t) = U_n(t + iT_p)$, $n = 0, \ldots, N-1$, $i \in \mathbb{Z}$,

$$U_n(t) = \begin{cases} 1 & t \le t_n \\ 0 & t_n < t \le T_p, \end{cases} \tag{2}$$

T_p being the time period, it is possible to express $I_n(t)$ in terms of the corresponding Fourier series

$$I_n(t) = \sum_{h=-\infty}^{\infty} A_{hn} e^{jh\omega_p t} \tag{3}$$

where $\omega_p = 2\pi/T_p$, $A_{hn} = \alpha_n a_{hn}$, and a_{hn} is the hth harmonic coefficient of $U_n(t)$ given by

$$a_{hn} = \frac{1}{T_p} \int_0^{T_p} U_n(t) e^{-jh\omega_p t} dt. \tag{4}$$

By substituting (3) in (1), the far field pattern radiated by the array appears to be the summation of an infinite number of harmonic contributions. More specifically, the central frequency beam is given by

$$F^{(0)}(\theta, t) = e^{j\omega_0 t} \sum_{n=0}^{N-1} \alpha_n a_{0n} e^{jnu}, \tag{5}$$

while the sideband radiations turns out to be

$$F_{SR}(\theta, t) = \sum_{h=-\infty (h\neq 0)}^{\infty} F^{(h)}(\theta, t) \tag{6}$$

where $F^{(h)}(\theta, t) = [\sum_{n=0}^{N-1} A_{hn} e^{jnu}] e^{j(h\omega_p + \omega_0)t}$.

As regards to the losses due to SRs, they can be analytically quantified according to the following closed form [4]

$$\mathcal{P}^{SR}(\underline{\alpha}, \underline{\tau}) = \sum_{n=0}^{N-1} \left\{ |\alpha_n|^2 \tau_n (1 - \tau_n) \right\} + \sum_{m,n=0 (m\neq n)}^{N-1} \left\{ \Re\left\{ \alpha_m \alpha_n^* \right\} \operatorname{sinc}\left[k(z_m - z_n) \right] (\tau_{mn} - \tau_m \tau_n) \right\} \tag{7}$$

0018-926X/$26.00 © 2010 IEEE

where $\Re\{\cdot\}$ and the apex * indicate the real part and complex conjugation, respectively. Moreover, $\underline{\tau} = \{\tau_n; n = 0, \ldots, N-1\}$ is the set of normalized switch-on times whose nth element is defined as $\tau_n = t_n/T_p$, while

$$\tau_{mn} = \begin{cases} \tau_n & if\ \tau_n \leq \tau_m \\ \tau_m & otherwise. \end{cases} \tag{8}$$

Therefore, it turns out that the SR power losses can be minimized by properly setting the values of the static excitations, $\underline{\alpha}$, as well as the durations of the time pulses, $\underline{\tau}$. However, since we are interested in synthesizing antennas with a low number of control parameters, uniform and isophoric excitations (i.e., $\alpha_n = 1$, $n = 0, \ldots, N-1$) are assumed. Only the durations of the switch-on times are then optimized by means of an iterative (k being the iteration index) PSO-based strategy aimed at minimizing the following cost function

$$\Psi(\underline{\tau}) = w_{SLL}\Psi^{SLL}(\underline{\tau}) + w_P\mathcal{P}_k^{SR}. \tag{9}$$

The first term in (9), $\Psi^{SLL} = H[SLL^{ref} - SLL_k](|SLL^{ref} - SLL_k|^2/|SLL^{ref}|^2)$, models a constraint on the array pattern at ω_0 and quantifies the distance between the current, SLL_k, and the desired sidelobe level, SLL^{ref}, while the latter is related to the power losses. Moreover, w_{SLL} and w_P are real weight coefficients and $H(\cdot)$ is the Heaviside step function.

As regards to the PSO-based minimization, the algorithm starts from randomly chosen guess values and updates at each iteration the set of S trial solutions, $\underline{\tau}_k^{(s)}$, $s = 1, \ldots, S$, as well as the corresponding PSO velocities, $\underline{v}_k^{(s)}$, $s = 1, \ldots, S$, as follows [11]

$$\begin{aligned} \underline{v}_k^{(s)} &= e\underline{v}_{k-1}^{(s)} + C_1 r_1 \left(\underline{p}_k^{(s)} - \underline{\tau}_{k-1}^{(s)}\right) + C_2 r_2 \left(\underline{g}_k - \underline{\tau}_{k-1}^{(s)}\right) \\ \underline{\tau}_k^{(s)} &= \underline{\tau}_{k-1}^{(s)} + \underline{v}_k^{(s)}, \quad s = 1, \ldots, S \end{aligned} \tag{10}$$

where e (*inertial weight*), C_1 (*cognitive acceleration*), and C_2 (*social acceleration*) are the PSO control parameters. Moreover, r_1 and r_2 are two random variables having uniform distribution in the range [0:1]. Furthermore, $\underline{p}_k^{(s)} = \arg\{min_{q=1,\ldots,k}[\Psi(\underline{\tau}_q^{(s)})]\}$ and $\underline{\tau}_k^{opt} = \arg\{min_{s=1,\ldots,S}[\Psi(\underline{p}_k^{(s)})]\}$ are the so-called *personal best* solution and *global best* solution, respectively. The process is iterated until a convergence criterion based either on a maximum number of iterations K or the following stationary condition

$$\frac{\left|K_{window}\Psi\left(\underline{\tau}_k^{opt}\right) - \sum_{q=1}^{K_{window}}\Psi\left(\underline{\tau}_{k-q}^{opt}\right)\Psi_l^{opt}\right|}{\Psi\left(\underline{\tau}_k^{opt}\right)} \leq \eta \tag{11}$$

holds true. In (11), K_{window} and η are a fixed number of iterations and a user-defined numerical threshold, respectively.

III. Numerical Results

This section is devoted to give some indications on the effectiveness of the proposed approach in minimizing the power losses associated to the SRs, while synthesizing a fixed-SLL pattern at the carrier frequency. Towards this purpose, some representative examples are reported and discussed also in a comparative fashion. Comments on the relationship between SR minimization, performance (i.e., SLL) and complexity of the synthesized array are given, as well.

Let us consider a linear array of $N = 30$ elements equally-spaced by $d = 0.7\lambda$. The same experiment has been previously dealt with in [10] with the aim of minimizing the sideband levels (SBLs) at $h = 1$, 2, while keeping a desired SLL at $\omega = \omega_0$. In [10], the optimization has been carried out by means of a Simulated Annealing (SA) approach by setting $SLL^{ref} = -20$ dB and $SBL^{ref} = -30$ dB, respectively. The synthesized solution [10] fulfills both requirements

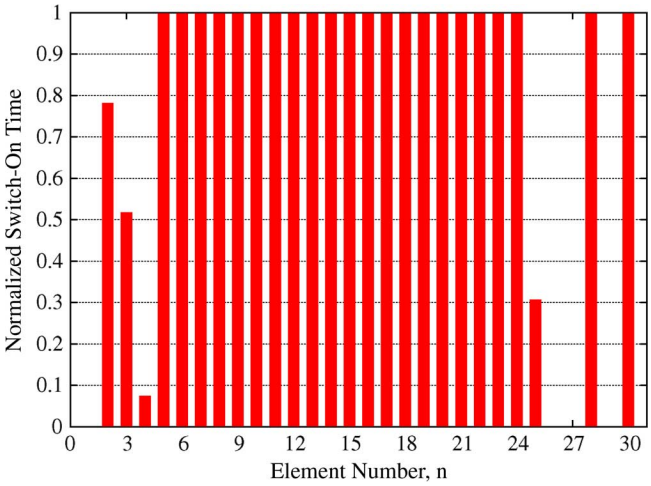

Fig. 1. *SR Minimization* ($N = 30$, $d = 0.7\lambda$)—Switch-on time sequence synthesized with the PSO-based approach.

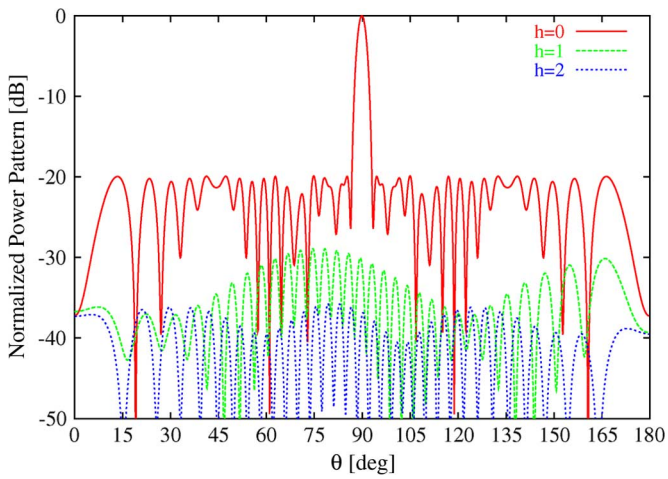

Fig. 2. *SR Minimization* ($N = 30, d = 0.7\lambda$)—Normalized power patterns at the carrier frequency ($h = 0$) and related to the sideband radiations ($h = 1, 2$) in correspondence with the pulse sequence in Fig. 1.

(i.e., $SLL_{SA} = -20$ dB, $SBL_{SA}^{(1)} = -30.2$ dB, and $SBL_{SA}^{(2)} = -35.1$ dB) by time-modulating only 9 elements over 30 and the power wasted in the sidelobe radiations amounts to $\mathcal{P}_{SA}^{SR} = 3.89\%$ of the total input power. The directivity and the feed-network efficiency computed through the relationships in [12] are equal to $D_{SA}^T = 15.14$ dB and $\eta_{SA}^f = 0.82$, respectively.

As far as the PSO-based method is concerned, a swarm of $S = 10$ particles (i.e., trial solutions) has been chosen and the control parameters have been set to $w = 0.4$, $C_1 = C_2 = 2.0$, and $K = 1000$. Moreover, a uniform weighting has been assumed in (9) (i.e., $w_{SLL} = w_P = 1.0$). The numerical simulations have been run on a 3 GHz PC with 1 GB of RAM and the convergence has been reached after $K_{end} = 761$ iterations with a total and average (per iteration) CPU time equal 113.39 [sec] and 0.149 [sec], respectively. The time sequence synthesized at $k = K_{end}$ is shown in Fig. 1 while the patterns afforded at the carrier frequency [(5)] and the first two harmonic patterns [(6)—$h = 1, 2$] are shown in Fig. 2. As it can be noticed (Fig. 1), only 4 elements are time modulated (versus 9 in [10]) and the same performances of the SA-based approach have been obtained neglecting the elements 1, 26, 27, and 29, which are always turned off.

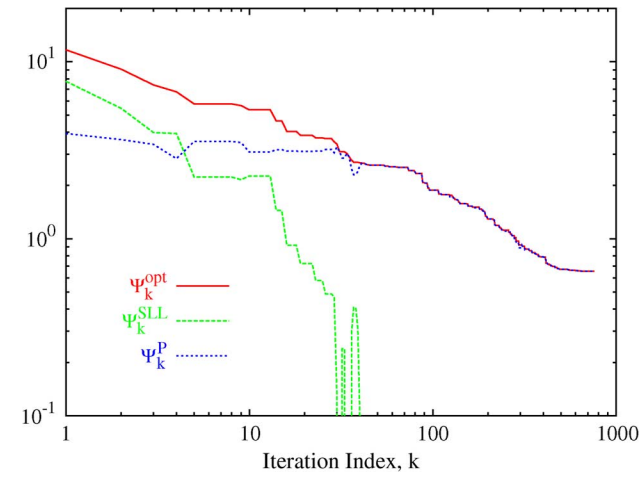

Fig. 3. *SR Minimization* ($N = 30, d = 0.7\lambda$)—Behavior of the cost function and its terms during the iterative PSO-based minimization.

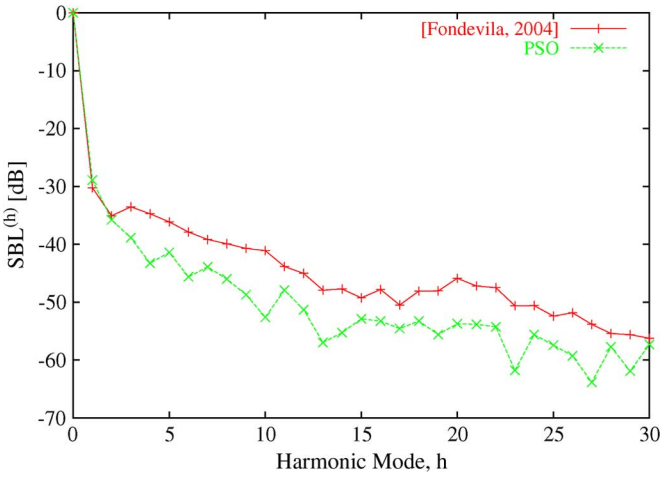

Fig. 4. *SR Minimization* ($N = 30, d = 0.7\lambda$)—Behavior of the sideband levels $SBL^{(h)}$ when $h \in [0, 30]$. Reference [10] and values computed with the PSO-optimized pulse sequence in Fig. 2.

As regards to the fulfillment of the synthesis constraints, Fig. 3 shows the behavior of $\Psi_k^{opt} = \Psi(\underline{\tau}_k^{opt})$ and the values of the two terms in (9). As expected, the PSO solution widely fulfils the user constraint on the SLL at the convergence [i.e., $\Psi^{SLL}(K_{end}) < 10^{-6}$], when the stationary condition on the value of the cost function is reached. Concerning the SR, although the sideband level of the first harmonic term of the PSO solution is higher than that synthesized with the SA approach (i.e., $SBL_{PSO}^{(1)} = -28.9$ dB vs. $SBL_{SA}^{(1)} = -30.2$ dB—Fig. 4), the amount of power losses in the SRs turns out to be lower since $\mathcal{P}_{PSO}^{SR} = 3.57\%$. Such a result points out that a suitable strategy based on the direct minimization of the SR, instead of the optimization of the SBLs [5], [8]–[10], seems to be more effective in reducing power losses. On the other hand, it should be noticed that the proposed techniques also guarantees satisfactory SBLs since, besides the first harmonic ($h = 1$), $SBL_{PSO}^{(h)} < SBL_{SA}^{(h)}$ for $h \geq 2$. As a matter of fact, the reduction of the SBL ranges from a minimum of $\Delta_{min}^{SBL} = 0.7$ dB to a maximum equal to $\Delta_{max}^{SBL} = 11.5$ dB, with an average value of around $\Delta_{av}^{SBL} = 6.2$ dB. Conversely, the directivity as well as the feed-network efficiency slightly reduce to $D_{PSO}^{T} = 14.94$ dB and $\eta_{PSO}^{f} = 0.79$.

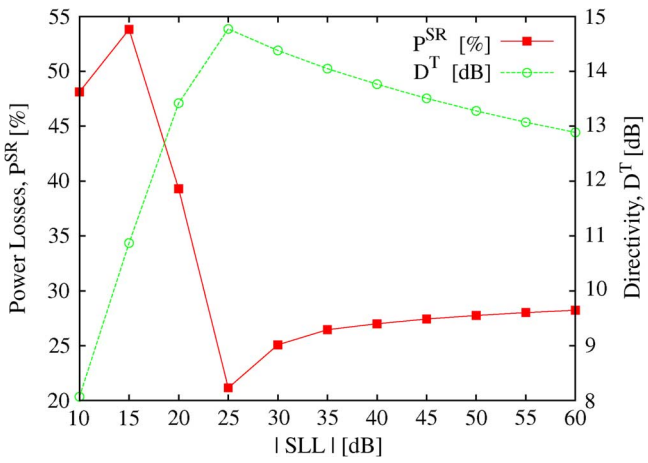

Fig. 5. *Performance Analysis* ($N = 30, d = 0.7\lambda$)—Behavior of the power losses $\mathcal{P}^{SR}$ and directivity D^T versus the SLL for Dolph-Chebyshev patterns [13].

Finally, Fig. 5 gives some indications on the trade-off between antenna performance (i.e., directivity and SLL) and associated power losses, $\mathcal{P}^{SR}$, when considering Dolph-Chebyshev distributions [13]. As expected, it is worth noting that there is an inverse relationship between the amount of power losses and the maximum directivity for time-modulated linear arrays.

IV. Conclusion

In this communication, an innovative approach for the synthesis of time-modulated arrays has been proposed. In order to reduce the power losses, a PSO-based optimization strategy has been adopted to minimize a closed-form relationship, which takes into account the whole sideband radiations in a direct way thus avoiding the computationally-expensive evaluation of the infinite set of harmonic patterns. Thanks to these key-features, the proposed technique represents an improvement with respect to state-of-the-art methods in terms of simplicity and efficiency as shown by some representative results.

Further investigations will concern with the extension of the PSO-based strategy to the synthesis of real-time adaptive systems suitable for communications as well as for the suppression of jamming signals.

References

[1] H. E. Shanks and R. W. Bickmore, "Four-dimensional electromagnetic radiators," *Canad. J. Phys.*, vol. 37, pp. 263–275, Mar. 1959.

[2] W. H. Kummer, A. T. Villeneuve, T. S. Fong, and F. G. Terrio, "Ultra-low sidelobes from time-modulated arrays," *IEEE Trans. Antennas Propag.*, vol. 11, no. 6, pp. 633–639, Nov. 1963.

[3] R. W. Bickmore, "Time versus space in antenna theory," in *Microwave Scanning Antennas*, R. C. Hansen, Ed. Los Altos, CA: Peninsula, 1985, vol. III, ch. 4.

[4] J. C. Brégains, J. Fondevila, G. Franceschetti, and F. Ares, "Signal radiation and power losses of time-modulated arrays," *IEEE Trans. Antennas Propag.*, vol. 56, no. 6, pp. 1799–1804, Jun. 2008.

[5] S. Yang, Y. B. Gan, A. Qing, and P. K. Tan, "Design of a uniform amplitude time modulated linear array with optimized time sequences," *IEEE Trans. Antennas Propag.*, vol. 53, no. 7, pp. 2337–2339, Jul. 2005.

[6] A. Tennant and B. Chambers, "Time-switched array analysis of phase-switched screens," *IEEE Trans. Antennas Propag.*, vol. 57, no. 3, pp. 808–812, Mar. 2009.

[7] J. Fondevila, J. C. Brégains, F. Ares, and E. Moreno, "Application of time modulation in the synthesis of sum and difference patterns by using linear arrays," *Microw. Opt. Technol. Lett.*, vol. 48, pp. 829–832, 2006.

[8] S. Yang, Y. B. Gan, and A. Qing, "Sideband suppression in time-modulated linear arrays by the differential evolution algorithm," *IEEE Antennas Wireless Propag. Lett.*, vol. 1, pp. 173–175, 2002.
[9] S. Yang, Y. B. Gan, and P. K. Tan, "A new technique for power-pattern synthesis in time-modulated linear arrays," *IEEE Antennas Wireless Propag. Lett.*, vol. 2, pp. 285–287, 2003.
[10] J. Fondevila, J. C. Brégains, F. Ares, and E. Moreno, "Optimizing uniformly excited linear arrays through time modulation," *IEEE Antennas Wireless Propag. Lett.*, vol. 3, pp. 298–301, 2004.
[11] J. Kennedy, R. C. Eberhart, and Y. Shi, *Swarm Intelligence*. San Francisco, CA: Morgan Kaufmann, 2001.
[12] S. Yang, Y. B. Gan, and P. K. Tan, "Evaluation of directivity and gain for time-modulated linear antenna arrays," *Microw. Opt. Technol. Lett.*, vol. 42, no. 2, pp. 167–171, Jul. 2004.
[13] C. L. Dolph, "A current distribution for broadside arrays which optimizes the relationship between beam width and sidelobe level," *Proc. IRE*, vol. 34, pp. 335–348, 1946.

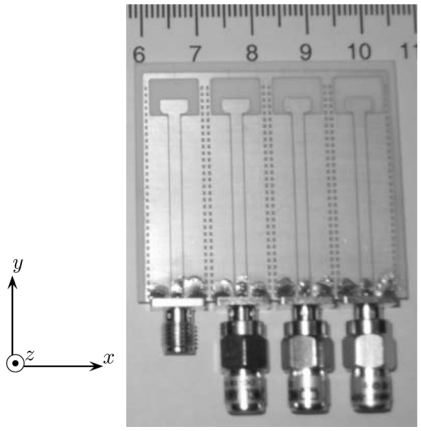

Fig. 1. Linear array of CPW fed, printed, loop antennas.

Experimental Validation of a Linear Array Consisting of CPW Fed, UWB, Printed, Loop Antennas

F. Muge Tanyer-Tigrek, Ioan E. Lager, and Leonardus P. Ligthart

***Abstract*—The linear array performance of an ultrawideband (UWB), coplanar waveguide (CPW) fed, printed, loop antenna is investigated by means of simulations and measurements. The UWB properties of the array are demonstrated by synthesizing the array reflection coefficient, starting from the simulated and measured scattering matrices. The array is proven to have a $\mathrm{VSWR} \leqslant 2$ fractional impedance bandwidth of 64%, stretching between 7 GHz and 13.6 GHz. The performance of a complete, non-scanning, broadside array are examined by feeding the array via a Wilkinson power divider. The study is completed by radiation pattern measurements that show stable co-polar and low cross-polar characteristics over the operational bandwidth.**

***Index Terms*—Antenna measurements, linear arrays, printed antenna, ultrawideband (UWB) antenna.**

I. Introduction

UWB technology is regarded as one of the most promising high data rate technologies. However, there are still challenges in making this technology live up to its full potential. One of the challenges is the design of the UWB antennas which have become the topic of continued investigation in the fields of wireless communications, due to such attractive features as transmitting and/or receiving electromagnetic energy in shorter duration and avoiding both frequency and space dispersion.

The antennas used for the UWB technology should satisfy certain specifications. First of all, they should transmit short pulses, meaning that the antenna must cover a large bandwidth in order to keep the ringing effects on the transmitted pulse at an acceptable level. Secondly, the input impedance of the antennas should be well matched to the transmitter and receiver for an efficient power transfer. Ideally, the pattern and the impedance matching should be stable across the entire band. In some applications, scanning the beam is required, which is the particular challenge in the UWB area and, thus, the antenna elements need being embedded in array environments. In such cases, the grating lobes free scanning requires the UWB elements to have small electrical sizes.

Many UWB antenna elements are known in the literature [1]–[6] and some of them have indeed electrically small sizes. However, their suitability for being employed in (linear) array requires their UWB properties to be maintained when brought in array environments, a topic that was not clearly elucidated. In this contribution, the performance of a linear array, the elements of which evolved from the tulip-loop antenna described in [4], is investigated for the first time. A method for calculating the array input reflection coefficient by using the simulated and measured scattering matrices of the array is proposed. Detailed array radiation pattern results obtained by both aggregating individual element characteristics and corporate feeding measurements are also reported. The account now proceeds by introducing the relevant array. The device's adequate UWB characteristics are demonstrated in Section III by a twofold study of the array impedance matching and, then, in Section IV by reporting radiation pattern measurements. The work is finalized by drawing some conclusions.

II. Investigated Array Structure

The linear array antenna under study employs the tulip-loop antenna presented in [4]. The individual elements have a width of 11 mm, including the metallic walls enclosing the loop itself. The tulip loop antenna has a $\mathrm{VSWR} \leqslant 2$ impedance bandwidth of 83%, stretching between 6 GHz and 14.5 GHz and stable radiation patterns within its impedance bandwidth. This antenna is investigated in detail in [4].

In view of studying their behavior in an array environment, the CPW fed printed loop antennas are assembled in a four elements, linear array (see Fig. 1). As clearly stated in [4], the employed radiators are characterized by a (practically) omnidirectional radiation in the xOz plane, recommending this plane for ensuring adequate scannable array operation. Consequently, the results reported in this work concern the xOz plane, only. For examining the far field radiation properties in this plane, a polar reference frame is employed, the polar angle $\vartheta (0^\circ \leqslant \vartheta < 360^\circ)$ measuring the trigonometric rotation around the Oy-axis, with the Oz-axis taken as reference (see Fig. 1). The array antenna has

Manuscript received February 19, 2009; revised August 25, 2009. Date of manuscript acceptance September 20, 2009; date of publication January 22, 2010; date of current version April 07, 2010.

The authors are with the International Research Centre for Telecommunications and Radar (IRCTR), Faculty of Electrical Engineering, Mathematics and Computer Science, Delft University of Technology, 2628 CD Delft, The Netherlands (e-mail: F.M.Tanyer-Tigrek@tudelft; i.e.lager@tudelft.nl; l.p.ligthart@tudelft.nl).

Color versions of one or more of the figures in this communication are available online at http://ieeexplore.ieee.org.

Digital Object Identifier 10.1109/TAP.2010.2041151

0018-926X/$26.00 © 2010 IEEE